Phytochemistry 151 (2018) 32–41

Contents lists available at ScienceDirect

Phytochemistry

journal homepage: www.elsevier.com/locate/phytochem

Hebecarposides A–K, antiproliferative lanostane-type triterpene glycosides from the leaves of *Lyonia ovalifolia* var. *hebecarpa*

Yang Teng [a, b, 1], Hanqi Zhang [a, 1], Junfei Zhou [a], Guanqun Zhan [a], Guangmin Yao [a, *]

[a] Hubei Key Laboratory of Natural Medicinal Chemistry and Resource Evaluation, School of Pharmacy, Tongji Medical College, Huazhong University of Science and Technology, Wuhan 430030, People's Republic of China
[b] College of Pharmacy, Jiamusi University, Jiamusi 154007, People's Republic of China

ARTICLE INFO

Article history:
Received 29 January 2018
Received in revised form
18 March 2018
Accepted 31 March 2018

Keywords:
Lyonia ovalifolia var. *hebecarpa*
Ericaceae
Lanostane-type triterpene glycosides
$Mo_2(OAc)_4$–induced ECD
Absolute configuration
Antiproliferative activity

ABSTRACT

Eleven previously undescribed lanostane-type triterpene glycosides, hebecarposides A–K, were isolated from the leaves of *Lyonia ovalifolia* var. *hebecarpa* (Ericaceae), along with two known analogues, lyonifolosides L and O. The structures of hebecarposides A–K were established by extensive spectroscopic analysis and chemical methods, and the absolute configuration of C-24 in hebecarposides A and E was determined to be *S* and *R*, respectively, by a $Mo_2(OAc)_4$–induced electronic circular dichroism method. This is the first report of the presence of lanostane-type triterpene glycosides in *L. ovalifolia* var. *hebecarpa*. All compounds were evaluated for their antiproliferative activities against five cancer cell lines, SMMC-7721, HL-60, SW480, MCF-7, and A-549, and a normal epithelial cell line BEAS-2B, and none of them showed general cytotoxity to the normal cell line BEAS-2B. Interestingly, hebecarposides C, D, G, and K selectively inhibited the proliferation of HL-60 and SMMC-7721 cell lines, and hebecarposides C and D showed significant anti-proliferative activities against A-549 cell lines than the positive control, *cis*-platin. In addition, hebecarposides C and H exhibited more potent anti-proliferative activities against MCF-7 than *cis*-platin.

1. Introduction

Lanostane (also known as 4,4,14-trimethylcholestane)-type triterpenoids possessing a 6/6/6/5 tetracyclic carbon ring system and eight methyls are widely distributed in mushrooms (mainly *Ganoderma*) and plants (Duru and Tel, 2015; Hamid et al., 2015; Isaka et al., 2017; Jin et al., 2014; Tohtahon et al., 2017). Although lanostane triterpene glycosides are the main components of sea cucumbers (Holothurioidea and Echinodermata) and mushrooms (Aminin et al., 2014; Kalinin et al., 2015; Lee et al., 2012), they are relatively rare in plants, and only reported from Liliaceae (Adinolfi et al., 1993; Ono et al., 2011; Ori et al., 2003a), Hyacinthaceae (Ori et al., 2003b), Verbenaceae (Okwu and Offiong, 2009), Leguminosae (Mamedova et al., 2003), and Ericaceae (Lv et al., 2016). Ericaceae plants are famous for their beautiful flowers and their structurally intriguing and bioactive diterpenoids components (Zhang et al., 2013, 2015; Zhou et al., 2017a, 2017b; 2018a, 2018b). However, studies of Ericaceae triterpenoids are not thorough, and the main triterpene skeletons are ursane, oleanane, lupane (Bukreyeva et al., 2013; Dai and Yu, 2005; Huang et al., 2007; Way et al., 2014; Yao et al., 2006), and dammarane (Dai and Yu, 2005). Recently, Lv et al. (2016) reported the isolation of lanostane and cycloartane triterpene glycosides with potent antiviral activity from the twigs and leaves of *Lyonia ovalifolia*.

Lyonia is a small genus of Ericaceae family, and is mainly distributed in Eastern Asia and North America. There are about 35 species of *Lyonia* in the world, and only six species and five varieties in China. *Lyonia ovalifolia* var. *hebecarpa* (Franch. ex F.B. Forbes & Hemsl.) Chun (Ericaceae) is endemic to China, and is mainly distributed in Jiangsu, Anhui, Zhejiang, Guangdong, Guangxi, and Yunnan provinces (Editorial Committee of the Flora of China, 1991). The branches and leaves are used as a folk medicine for an astringent agent. Phytochemical studies on *L. ovalifolia* var. *hebecarpa* are rare, only a megastigmane sesquiterpene glycoside and two steroids were reported (Wang et al., 2001). In a course of search for bioactive compounds from Ericaceae plants (Zhang et al., 2013, 2015; Zhou et al., 2017a, 2017b; 2018a, 2018b), the leaves of *L. ovalifolia* var. *hebecarpa* were investigated, leading to the isolation

* Corresponding author.
E-mail address: gyap@mail.hust.edu.cn (G. Yao).
[1] Y. Teng and H. Zhang contributed equally.

https://doi.org/10.1016/j.phytochem.2018.03.012
0031-9422/

of eleven previously undescribed lanostane triterpene glycosides (**1**–**11**) and two known analogues (**12** and **13**) (Fig. 1). This is the first report of lanostane triterpene glycosides from *L. ovalifolia* var. *hebecarpa*. In this paper, the isolation, structure elucidation, and antiproliferative activities of thirteen lanostane triterpene glucosides (**1**–**13**) are described.

2. Results and discussion

The air-dried leaves of *L. ovalifolia* var. *hebecarpa* were extracted with 95% aqueous EtOH. The crude extract was suspended in H_2O and then partitioned excessively with petroleum ether and chloroform. The chloroform fraction was repeatedly subjected to silica gel, reversed phase (RP) C_{18} silica gel, and Sephadex LH−20 column chromatography, as well as HPLC on a semipreparative XB−C_{18} column to yield eleven previously undescribed lanostane-type triterpene glycosides (**1**–**11**) and two known analogues (**12** and **13**). Known lanostane-type triterpene glycosides were identified to be lyonifolosides L (**12**) and O (**13**) (Lv et al., 2016), respectively, by comparison of their spectroscopic data with those reported in the literature.

Hebecarposide A (**1**) was obtained as a white amorphous power. Its molecular formula was established as $C_{35}H_{58}O_9$ by the HRESIMS at *m/z* 645.3978 $[M + Na]^+$ (calcd for $C_{35}H_{58}O_9Na$, 645.3979) and ^{13}C NMR data, indicating seven indices of hydrogen deficiency. The ^1H NMR data of **1** (Table 1) showed resonances for seven methyl groups at δ_H 0.82 (3H, s, CH_3-18), 1.07 (3H, s, CH_3-19), 0.96 (3H, d, $J = 6.2$ Hz, CH_3-21), 1.16 (3H, s, CH_3-26), 1.13 (3H, s, CH_3-27), 0.98 (3H, s, CH_3-28), and 0.90 (3H, s, CH_3-29), an oxymethine at δ_H 3.39 (1H, br s, H-3β), and an arabinopyranosyl unit at δ_H 4.20 (1H, d, $J = 6.2$ Hz, H-1′), 3.53 (1H, m, H-2′), 3.52 (1H, m, H-3′), 3.81 (1H, dd, $J = 4.0$, 2.9 Hz, H-4′), 3.48 (1H, dd, $J = 12.4$, 1.2 Hz, H-5′a), and 3.85 (1H, dd, $J = 12.4$, 2.9 Hz, H-5′b) (Lv et al., 2016). The ^{13}C NMR and DEPT data of **1** (Table 2) exhibited a total of 36 carbon resonances corresponding to seven methyls, ten methylenes, three methines including two oxymethines at δ_C 82.2 (C-3) and 80.6 (C-24), four quaternary carbons, one oxygenated tertiary carbon at δ_C 74.1 (C-25), two tertiary sp^2 carbons at δ_C 128.9 (C-8) and 141.9 (C-9), a carboxyl group at δ_C 180.5 (C-30), and an arabinopyranosyl unit at δ_C 102.1 (C-1′), 72.6 (C-2′), 74.5 (C-3′), 69.9 (C-4′), and 67.0 (C-5′) (Lv et al., 2016). Apart from three indices of hydrogen deficiency occupied by a double bond, a carboxyl group, and an arabinopyranosyl unit, the remaining four indices of hydrogen deficiency suggested that compound **1** is a tetracyclic triterpene glycoside. The NMR data of **1** resembled those of **12** (lyonifoloside L) (Lv et al., 2016), except for an arabinopyranosyl unit in **1**, instead of a glucopyranosyl unit in **12**. The glycosidation at C-3 was proved by the cross-peaks from the anomeric proton H-1′ to C-3 (δ_C 82.2) and from H-3 to the anomeric carbon C-1' (δ_C 102.1) in the HMBC spectrum of **1**. The planar structure of **1** was confirmed by $^1H-^1H$ COSY, HSQC, and HMBC analyses (Fig. 2). The broad single peak of H-3 (δ_H 3.39, br s) in the ^1H NMR established its equatorial position in the chair conformation of the cylcohexane in ring A (Fig. 2), and H-3 was in a β-orientation (Lv et al., 2016). NOESY analysis (Fig. 3) and comparison of NMR data with **12** suggested that the relative configuration of **1** is same to **12**, ignoring the sugar moieties.

To determine the absolute configuration of the arabinopyranose, **1** was hydrolyzed by 2 mM HCl to obtain the sugar, and then, the trimethylsilylthiazolidine derivatives of the sugar and standards, D and L-arabinose, were prepared. By comparing the retention times of these three trimethylsilylthiazolidine derivatives obtained from gas chromatography (GC), the absolute configuration of the arabinopyranose in **1** was determined to be L. The coupling constant of the anomeric hydrogen $J = 6.2$ Hz (δ_H 4.20, d, H-1′) established the α-arabinopyranosyl linkage in **1**. Due to the existence of a *vic*-diols unit in the side chain, a dimolybdenum tetraaccetate $[Mo_2(OAc)_4]$ −induced electronic circular dichroism (IECD) experiment was implemented to establish the absolute configuration of C-24 in **1** (Frelek et al., 2003; Gorecki et al., 2006, 2007; Snatzke et al., 1981). To eliminate the effects of the arabinose and carboxylic acid on the IECD, **1** was hydrolyzed by 0.6 mM TsOH·H_2O, instead of HCl, to afford the genuine aglycone **1a**, and then, **1a** was methylated with CH_3I to yield an ester **1b**. As shown in Fig. 4, the $Mo_2(OAc)_4$-induced ECD spectrum of the ester **1b** exhibited a positive Cotton effect at 316 nm, suggesting the *S* configuration of C-24 (Frelek et al., 2003; Gorecki et al., 2006, 2007; Snatzke et al.,

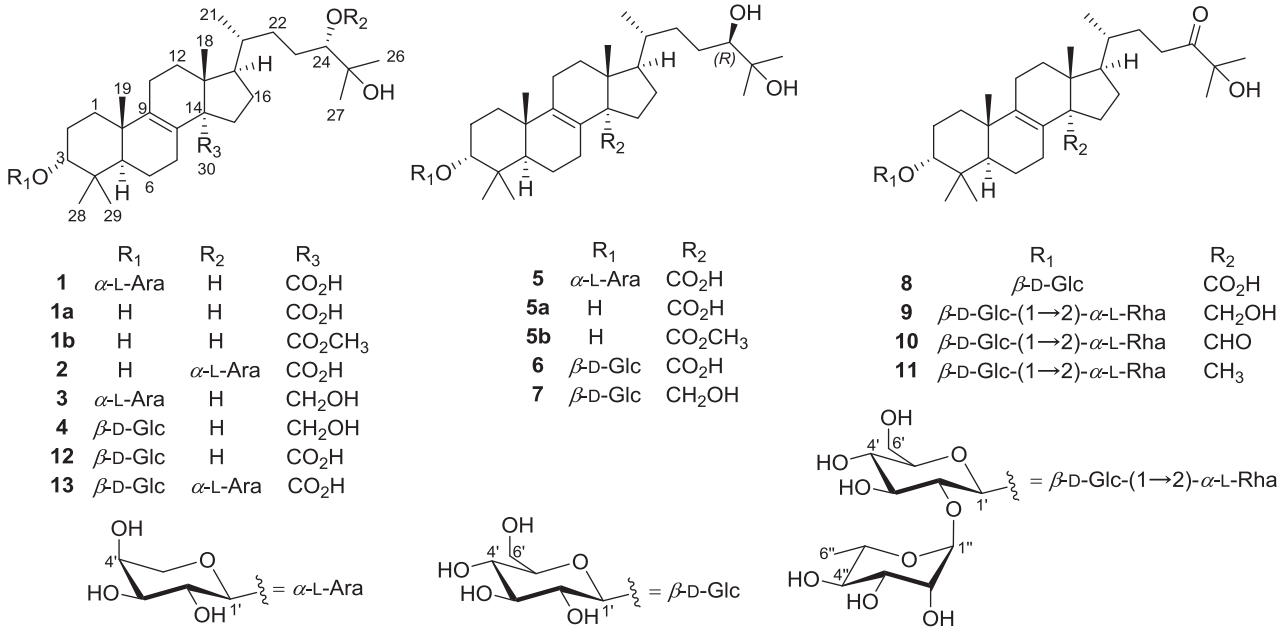

Fig. 1. Chemical structures of lanostane-type triterpene glycosides **1**–**13**.

Table 1
^{1}H NMR spectroscopic data for compounds **1**–**5b** (δ in ppm, J in Hz, and 400 MHz).

No.	**1**[a]	**1a**[a]	**1b**[a]	**2**[a]	**3**[b]	**4**[a]	**5**[b]	**5a**[a]	**5b**[a]
1α	1.41, m	1.29, m	1.30, m	1.38, m	1.46, m	1.39, m	1.54, m	1.29, m	1.46, m
1β	2.10, m	1.68, m	1.67, m	2.09, m	2.07, m	2.08, m	2.04, m	1.68, m	1.63, m
2α	1.95, m	1.96, m	1.90, m	1.95, m	1.97, m	1.74, m	1.99, m	1.93, m	1.96, m
2β	1.61, m	1.59, m	1.56, m	1.55, m	1.57, m	1.62, m	1.84, m	1.59, m	1.58, m
3β	3.39, br s	3.35, br s	3.35, br s	3.35, overlap	3.42 br s	3.52, br s	3.64, overlap	3.35, overlap	3.35, overlap
5α	1.63, m	1.62, m	1.60, m	1.62, m	1.76, m	1.75, m	1.95, m	1.62, m	1.57, m
6α	1.54, m	1.56, m	1.58, m	1.59, m	1.57, m	1.52, m	1.55, m	1.54, m	1.56, m
6β	1.63, m	1.62, m	1.65, m	1.65, m	1.63, m	1.61, m	1.62, m	1.61, m	1.62, m
7α	1.94, m	2.01, m	1.90, m	2.01, m	2.00, m	1.98, m	2.19, m	2.00, m	1.92, m
7β	2.08, m	2.07, m	2.07, m	2.09, m	2.08, m	2.08, m	2.33, m	2.08, m	2.07, m
11α	2.05, m	2.15, m	2.15, m	2.07, m	2.09, m	1.74, m	2.19, m	2.15, m	2.17, m
11β	2.13, m	2.25, m	2.25, m	2.17, m	2.10, m	2.16, m	2.37, m	2.26, m	2.22, m
12α	1.71, m	1.69, m	1.74, m	1.69, m	1.71, m	1.70, m	1.79, m	1.72, m	1,73, m
12β	2.20, m	2.32, m	2.17, m	2.21, m	2.22, m	2.19, m	2.78, m	2.32, m	2.28, m
15α	2.21, m	2.07, m	2.07, m	2.20, m	2.11, m	2.11, m	2.48, m	2.09, m	2.08, m
15β	1.56, m	1.57, m	1.56, m	1.55, m	1.55, m	1.57, m	1.70, m	1.49, m	1.55, m
16α	1.55, m	1.59, m	1.60, m	1.56, m	1.62, m	1.57, m	1.80, m	1.33, m	1.43, m
16β	2.08, m	2.09, m	2.07, m	2.09, m	2.05, m	2.06, m	2.46, m	2.09, m	2.05, m
17α	1.52, m	1.51, m	1.44, m	1.52, m	1.52, m	1.48, m	2.09, m	1.55, m	1.44, m
18β	0.82, s	0.81, s	0.82, s	0.81 s	0.74, s	0.72, s	0.94, s	0.82, s	0.82, s
19β	1.07, s	1.06, s	1.05, s	1.06 s	1.05, s	1.03, s	1.14, s	1.06, s	1.05, s
20β	1.46, m	1.47, m	1.46, m	1.46, m	1.42, m	1.41, m	1.67, s	1.49, m	1.49, m
21α	0.96, d (6.2)	0.96, d (6.4)	0.95, d (6.4)	0.96, d (5.4)	0.94, d (6.3)	0.94, d (6.1)	1.06, d, (5.2)	0.95, d (5.5)	0.95, d (5.5)
22a	1.70, m	1.49, m	1.52, m	1.47, m	1.72, m	1.70, m	1.65, m	1.49, m	1.45, m
22b	1.79, m	1.80, m	1.80, m	1.80, m	1.81, m	1.80, m	1.81, m	1.27, m	1.26, m
23a	1.50, m	1.46, m	1.47, m	1.51, m	1.46, m	1.46, m	1.69, m	1.45, m	1.49, m
23b	2.09, m	1.68, m	1.68, m	1.69, m	2.03, m	1.99, m	2.49, m	1.78, m	1.80, m
24	3.16, dd (10.2, 1.3)	3.15, dd (10.0, 1.2)	3.15, dd (10.0, 1.6)	3.10, d (8.0)	3.15, dd (10.0, 1.2)	3.14, dd (10.2, 1.2)	3.74, dd (10.0, 2.0)	3.21, dd (10.3, 0.9)	3.21, d (10.0, 0.8)
26	1.16, s	1.16, s	1.16, s	1.16, s	1.16, s	1.16, s	1.50, s	1.16, s	1.16, s
27	1.13, s	1.13, s	1.12, s	1.14, s	1.14, s	1.13, s	1.53, s	1.12, s	1.12, s
28α	0.98, s	0.94, s	0.94, s	0.94, s	0.94, s	0.99, s	1.15, s	0.94, s	0.94, s
29β	0.90, s	0.88, s	0.88, s	0.88, s	0.88, s	0.91, s	0.94, s	0.88, s	0.88, s
30a					3.50, overlap	3.49, overlap			
30b					3.33, overlap	3.32, overlap			
31			3.59, s						3.59, s
1′	4.20, d (6.2)			4.26, d (6.8)	4.26, d, (7.0)	4.30, d (7.6)	4.69, d (6.8)		
2′	3.53, m			3.56, m	3.54, m	3.15, m	4.3, m		
3′	3.52, m			3.53, m	3.55, m	3.34, m	4.14, dd (8.5, 3.3)		
4′	3.81, dd (4.0, 2.9)			3.88, ddd (3.9, 2.9, 1.3)	3.80, ddd (4.0, 2.8, 1.2)	3.23, m	4.34, m		
5′a	3.48, dd (12.4, 1.2)			3.55, m	3.50, m	3.21, m	3.75, m		
5′b	3.85, dd (12.4, 2.9)			3.88, dd (12.8, 2.9)	3.86, dd (12.4, 2.8)		4.26, m		
6′a						3.65, dd (11.8, 5.7)			
6′b						3.86, dd (11.8, 1.9)			

[a] Recorded in methanol-d_4.
[b] Recorded in pyridine-d_5.

1981), which was the same as **12** (Lv et al., 2016). Thus, the structure of compound **1** was identified as 3α-[(α-L-arabinopyranosyl)-oxy]-24(*S*),25-dihydroxylanost-8-en-30-oic acid.

Hebecarposide B (**2**), a white amorphous power, shared a same molecular formula of $C_{35}H_{58}O_9$ with **1** as determined by the HRESIMS at *m/z* 645.3966 $[M + Na]^+$ (calcd for $C_{35}H_{58}O_9Na$, 645.3979) and ^{13}C NMR data. The NMR data (Tables 1 and 2) of **2** were similar to **1**, and the main differences were that C-3 (δ_C 76.8) in **2** was shielded, compared to that (δ_C 82.2) in **1**, while C-24 (δ_C 89.5) in **2** was deshielded, compared to that in **1** (δ_C 80.6). Thus, the arabinopyranosyloxyl group should be located at C-24 in **2**, instead of C-3 in **1**. The HMBC correlations from the anomeric proton H-1' (δ_H 4.26, d, $J = 6.8$ Hz) of the arabinopyranose to C-24 (δ_C 89.5) and from H-24β (δ_H 3.10, dd, $J = 8.0$ Hz) to the anomeric carbon C-1' (δ_C 105.5) of the arabinopyranose confirmed this conclusion. The absolute configuration of the arabinopyranose unit in **2** was determined to be L by the same chemical method and GC analysis as **1**. The α-arabinopyranosyl linkage was deduced from the coupling constant ($J = 6.8$ Hz) of the anomeric proton H-1'. Therefore, the structure of compound **2** was determined to be 3α-[(α-L-arabinopyranosyl)-oxy]-24(*S*),25-dihydroxylanost-8-en-30-oic acid.

Hebecarposide C (**3**) was obtained as a white amorphous power. Its molecular formula was determined as $C_{35}H_{60}O_8$ by the HRESIMS (*m/z* 631.4193 $[M + Na]^+$, calcd for $C_{35}H_{60}O_8Na$, 631.4186) and ^{13}C NMR data. The NMR data (Tables 1 and 2) of **3** were similar to those of **1**, except for the presence of an oxymethylene (δ_H 3.50, 3.33, H_2-30; δ_C 68.7, C-30) in **3**, replacing of the carboxyl group (δ_C 180.5, C-30) in **1**. HMBC correlations from H_2-15 (δ_H 2.11, 1.55) to C-30 (δ_C 68.7) and from H_2-30 (δ_H 3.50, 3.33) to C-8 (δ_C 133.0), C-13 (δ_C 46.9), C-14 (δ_C 56.9), and C-15 (δ_C 26.6) confirmed the position of the oxygenated methylene C-30 (Fig. 2). Thus, compound **3** was identified as 3α-[(α-L-arabinopyranosyl)-oxy]-24(*S*),25,30-trihydroxylanost-8-ene.

Hebecarposide D (**4**), a white amorphous power, gave a

Table 2
^{13}C NMR spectroscopic data for compounds **1**–**5b** (δ in ppm and 100 MHz).

No.	**1**[a]	**1a**[a]	**1b**[a]	**2**[a]	**3**[b]	**4**[a]	**5**[b]	**5a**[a]	**5b**[a]
1	30.5	31.2	31.1	30.4	31.5	31.5	31.0	31.1	31.1
2	22.2	26.8	26.9	26.9	21.9	21.9	22.5	26.9	26.9
3	82.2	76.8	76.7	76.8	81.8	81.5	82.3	76.8	76.7
4	38.4	38.8	38.8	38.8	38.4	38.4	38.0	38.8	38.8
5	45.8	45.1	45.2	45.2	45.8	45.8	45.6	45.1	45.2
6	19.5	19.5	19.5	19.5	19.5	19.5	19.0	19.5	19.5
7	28.6	28.6	28.6	28.7	29.7	29.7	28.1	28.6	28.6
8	128.9	128.9	128.3	128.9	133.0	133.0	128.5	128.8	128.3
9	141.9	141.8	142.2	141.9	138.6	138.6	140.6	141.9	142.1
10	38.7	38.8	38.8	38.8	38.7	38.6	38.3	38.8	38.8
11	23.4	23.3	23.4	23.4	22.5	22.5	23.2	23.4	23.4
12	32.7	32.9	33.0	32.9	32.5	32.5	32.1	32.9	33.0
13	48.3	48.1	48.3	48.2	46.9	46.9	47.5	48.1	48.4
14	64.1	64.0	64.4	64.1	56.9	56.9	63.4	64.0	64.4
15	29.0	29.1	28.9	29.1	26.6	26.5	29.0	30.0	29.0
16	29.2	29.2	29.2	29.6	29.6	29.3	30.2	29.0	30.3
17	52.4	52.3	52.3	52.5	53.0	53.0	51.9	52.5	52.7
18	18.4	18.5	18.4	18.6	17.8	17.9	18.4	18.5	18.4
19	20.4	20.0	19.9	20.1	19.6	19.6	20.2	20.0	19.9
20	37.8	37.9	37.9	37.8	38.4	38.4	36.9	37.3	37.2
21	19.5	19.4	19.2	19.2	19.6	19.6	19.2	19.2	19.1
22	34.9	34.9	34.9	34.3	35.1	35.1	34.4	34.4	34.3
23	31.1	31.1	31.1	31.1	29.9	29.9	29.4	31.1	28.6
24	80.6	80.8	80.7	89.5	80.8	80.8	79.4	79.9	79.8
25	74.1	74.0	74.0	73.7	74.1	74.1	73.1	74.0	74.0
26	25.8	25.8	25.9	26.8	25.0	26.0	26.2	25.8	25.9
27	25.1	25.0	25.0	25.0	26.0	25.0	26.5	25.1	25.0
28	29.3	28.9	28.9	28.9	29.3	29.1	29.2	28.9	28.9
29	23.2	24.0	23.0	23.0	23.1	23.1	23.0	24.0	23.0
30	180.5	180.2	178.3	180.2	68.7	68.6	178.9	180.0	178.2
31			52.5						52.3
1′	102.1			105.5	101.7	101.0	103.2		
2′	72.6			72.9	72.8	75.4	72.5		
3′	74.5			74.5	74.6	78.4	75.1		
4′	69.9			70.0	70.0	72.2	69.7		
5′	67.0			67.5	67.1	78.1	67.0		
6′						63.2			

[a] Recorded in methanol-d_4.
[b] Recorded in pyridine-d_5.

molecular formula of $C_{35}H_{60}O_8$ as determined by HRESIMS (*m/z* 661.4289 $[M + Na]^+$, calcd for $C_{36}H_{62}O_9Na$, 661.4292) and ^{13}C NMR data. Based on the NMR spectroscopic data analysis (Tables 1 and 2), hebecarposide D (**4**) was inferred to be similar to **3**, except for their sugar moieties. NMR spectra of **4** showed resonances for a glucopyranosyl unit at δ_H 4.30 (1H, d, $J = 7.6$ Hz, H-1′), 3.15 (1H, m, H-2′), 3.34 (1H, m, H-3′), 3.23 (1H, m, H-4′), 3.21 (1H, m, H-5′), 3.65 (1H, dd, $J = 11.8$, 5.7 Hz, H-6′a), and 3.86 (1H, dd, $J = 11.8$, 1.9 Hz, H-6′b); δ_C 101.0 (C-1′), 75.4 (C-2′), 78.4 (C-3′), 72.2 (C-4′), 78.1 (C-5′), and 63.2 (C-6′) (Lv et al., 2016). HMBC correlations of H-3 (δ_H 3.52, br s) to C-1' (δ_C 101.0) and H-1' (δ_H 4.30, d, $J = 7.6$ Hz) to C-3 (δ_C 81.5) proved the glycosidation position at C-3. The absolute configuration of the glucopyranose in **4** was determined to be D by the same chemical method and GC analysis as **1**, and the coupling constant of anomeric proton $J = 7.6$ Hz (δ_H 4.30, d, H-1′) established the β-glucopyranosyl linkage in **4**. Hence, compound **4** was established as 3α-[(β-D-glucopyranosyl)-oxy]-24(*S*),25,30-trihydroxylanost-8-ene.

Hebecarposide E (**5**) was determined to possess a same molecular formula as **1** by the HRESIMS peak at *m/z* 645.4007 $[M + Na]^+$ (calcd for $C_{35}H_{58}O_9Na$, 645.3979) and ^{13}C NMR data. Comparison of their NMR data (Tables 1 and 2) revealed the deshielding of H-24α (δ_H 3.74, dd, $J = 10.0$, 2.0 Hz) and the shielding of C-24 (δ_C 79.4) in **5** than that (δ_H 3.16, dd, $J = 10.2$, 1.3 Hz, H-24; δ_C 80.6, C-24) in **1**. Thus, C-24 in compound **5** should have a different configuration from **1**. To determine the absolute configuration of C-24, compound **5** was hydrolyzed by 0.6 mM TsOH·H_2O to obtain the aglycone **5a**, which was then methylated with CH_3I to give the aglycone ester **5b**. The $Mo_2(OAc)_4$-induced ECD spectrum of **5b** (Fig. 4) showed a negative Cotton effect at 314 nm, which was opposite to that of **1b**. Thus, the absolute configuration of C-24 was established to be *R*. Accordingly, the structure of compound **5** was defined as 3α-[(α-L-arabinopyranosyl)-oxy]-24(*R*),25-dihydroxylanost-8-en-30-oic acid by 2D NMR analysis and the same chemical methods as **1**. Therefore, the chemical shifts of C-24 and H-24 may be used to assign its absolute configuration.

The molecular formula of hebecarposide F (**6**) was assigned as $C_{35}H_{60}O_{10}$ based on the HRESIMS (*m/z* 675.4136 $[M + Na]^+$, calcd for $C_{35}H_{60}O_{10}Na$ 675.4084) and ^{13}C NMR data. The NMR data (Tables 3 and 4) of **6** were similar to those of **5**, except for the typical resonances for a glucopyranosyl unit at δ_H 4.30 (d, $J = 7.7$ Hz, H-1′), 3.17 (m, H-2′), 3.38 (m, H-3′), 3.26 (m, H-4′), 3.24 (m, H-5′), 3.66 (dd, $J = 11.8$, 5.6 Hz, H-6′a), and 3.86 (dd, $J = 11.8$, 2.0 Hz, H-6′b) and δ_C 101.6 (C-1′), 75.2 (C-2′), 78.2 (C-3′), 72.1 (C-4′), 78.0 (C-5′), and 63.2 (C-6′) in **6**, replacing the α-L-arabinopyranosyl unit in **5**. Based on the cross peaks from H-1' (δ_H 4.30, d) to C-3 (δ_C 82.0) and H-3 (δ_H 3.50, br s) to C-1' (δ_C 101.6) in the HMBC spectrum, the glycosidation position was determined to be C-3 in **6** (Fig. 2). The absolute configuration of the glucopyranose in **6** was assigned to be D by the same chemical method and GC analysis as **1**, and the β-glucopyranosyl linkage was determined by the coupling constant of H-1' ($J = 7.7$ Hz). Thus, the structure of **6** was established as 3α-[(β-D-glucopyranosyl)-oxy]-24(*R*),25,30-trihydroxylanost-8-en-30-oic acid.

Hebecarposide G (**7**) had a molecular formula of $C_{36}H_{62}O_9$ as deduced by the HRESIMS at *m/z* 661.4316 $[M + Na]^+$ (calcd for 661.4292) and ^{13}C NMR data, indicating that it had one less index of hydrogen deficiency than **6**. The NMR data (Tables 3 and 4) of **7** showed similarities to those of **6**, and the major difference was the presence of an oxymethylene group (δ_H 3.47, 3.36, H_2-30; δ_C 68.6, C-30) in **7**, instead of the carboxyl group (δ_C 180.5, C-30) in **6**. In the HMBC spectrum of **7**, H_2-30 correlated to C-8 (δ_C 132.9), C-13 (δ_C 46.9), C-14 (δ_C 56.9), and C-15 (δ_C 26.5), proving the location of the oxymethylene group 30-CH_2OH at C-14 in **7** (Fig. 2). Hence, compound **7** was defined as 3α-[(α-L-arabinopyranosyl)-oxy]-24(*R*),25,30-trihydroxylanost-8-ene.

Hebecarposide H (**8**) was proved to have a molecular formula of $C_{36}H_{58}O_{10}$ by the HRESIMS peak at *m/z* 673.3913 $[M + Na]^+$ (calcd for $C_{36}H_{58}O_{10}Na$, 673.3928) and ^{13}C NMR data. The NMR data (Tables 3 and 4) of compound **8** were similar to those of **7**, except for that a ketone carbonyl (δ_C 218.0, C-24) in **8** replaced the oxymethylene group (δ_H 3.47, 3.36, H_2-30; δ_C 68.6, C-30) in **7**. HMBC correlations from H_3-26/H_3-27 (δ_H 1.29) to C-24 confirmed the location of the ketone carbonyl at C-24 (Fig. 2). Thus, compound **8** was determined as 3α-[(β-D-glucopyranosyl)-oxy]-25-hydroxy-24-oxolanost-8-en-30-oic acid.

Hebecarposide I (**9**) was isolated as a white amorphous power. The sodium adduct ion at *m/z* 805.4705 $[M + Na]^+$ in the HRESIMS and ^{13}C NMR data assigned a molecular formula of $C_{42}H_{70}O_{13}$ to **9**, suggesting nine indices of hydrogen deficiency. Comparison of their NMR data (Tables 3 and 4) revealed that compound **9** differed from **8** in the presence of an oxygenated methylene group (δ_H 3.97, 3.76, each d, $J = 10.2$ Hz, H_2-30; δ_C 68.1, C-30) in **9**, replacing the carboxyl group (δ_C 181.2, C-30) in **8**. Another major difference was the presence of an additional rhamnopyranosyl moiety (δ_H 6.50, s, H-1''; 4.80, dd, $J = 3.1$, 1.2 Hz, H-2''; 4.60, dd, $J = 9.3$, 3.1 Hz, H-3''; 4.26, m, H-4''; 4.74, dd, $J = 9.3$, 6.2 Hz, H-5''; 1.72, d, $J = 6.2$ Hz, H-6''; δ_C 101.3, C-1''; 72.9, C-2''; 72.0, C-3''; 74.5, C-4''; 69.9, C-5''; 19.1, C-6″) in **9**. The HMBC correlations from the anomeric proton H-1'' (δ_H 6.50, s) of the rhamnopyranosyl to C-2' (δ_C 76.6) of the glucopyranosyl unit suggested the location of the rhamnopyranosyl unit at C-2′ of the glucopyranosyl unit. The location of the oxymethylene

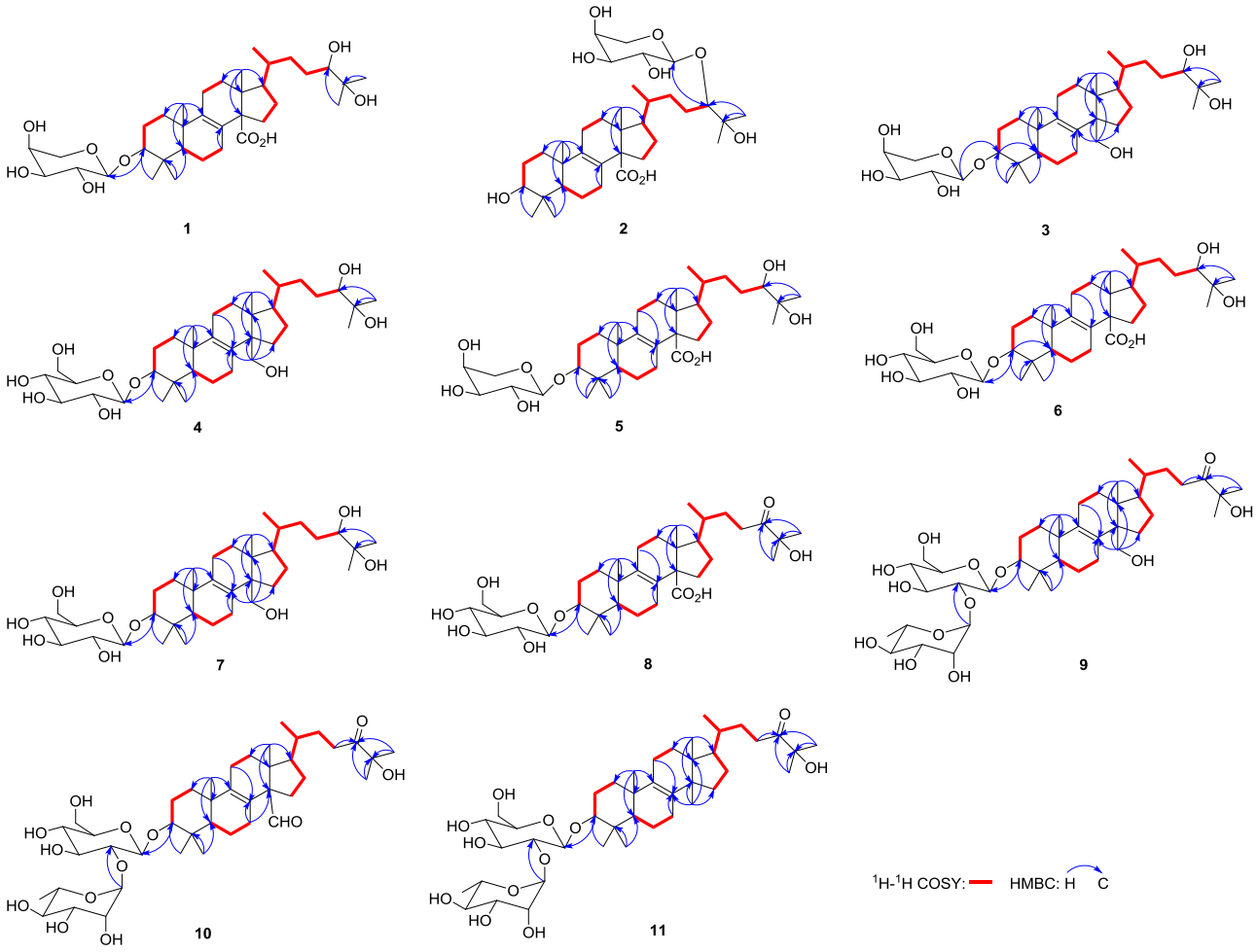

Fig. 2. ^{1}H–^{1}H COSY and key HMBC correlations of compounds **1**–**11**.

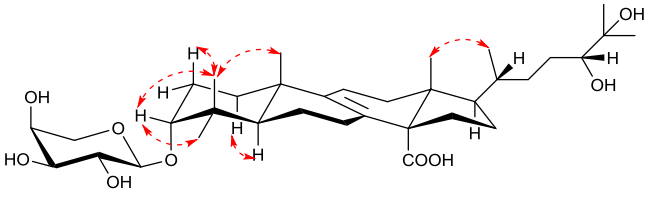

Fig. 3. Key NOESY correlations of compound **1**.

group 30-CH_2OH at C-14 was deduced from the HMBC correlations from H_2-30 (δ_H 3.97, 3.76, each d, $J = 10.2$ Hz, H_2-30) to C-8 (δ_C 123.9), C-13 (δ_C 46.2), and C-14 (δ_C 56.4) (Fig. 2). The absolute configurations of the arabinopyranose and glucopyranose were determined to be L and D, respectively, by the same chemical methods and GC analysis as **1**. Thus, compound **9** was defined as 3α-[α-L-arabinopyranosyl-(1 → 2)-(β-D-glucopyranosyl)-oxy]-25,30-dihydroxy-24-oxolanost-8-ene.

The HRESIMS peak at *m/z* 803.4526 $[M + Na]^+$ and ^{13}C NMR data established the molecular formula of hebecarposide J (**10**) to be $C_{42}H_{68}O_{13}$ (calcd for $C_{42}H_{68}O_{13}Na$, 803.4558). The NMR data (Tables 3 and 4) of **10** were similar to those of **9**, with the major difference of an aldehyde group (δ_H 10.16, s, H-30; δ_C 201.4, C-30) in **10**, instead of an oxymethylene group (δ_H 3.97, 3.76, each d, $J = 10.2$ Hz, H_2-30; δ_C 68.1, C-30) in **9**. HMBC cross-peaks of H-30 (δ_H 10.16, s) to C-8 (δ_C 122.3), C-13 (δ_C 46.4), and C-14 (δ_C 67.7) verified

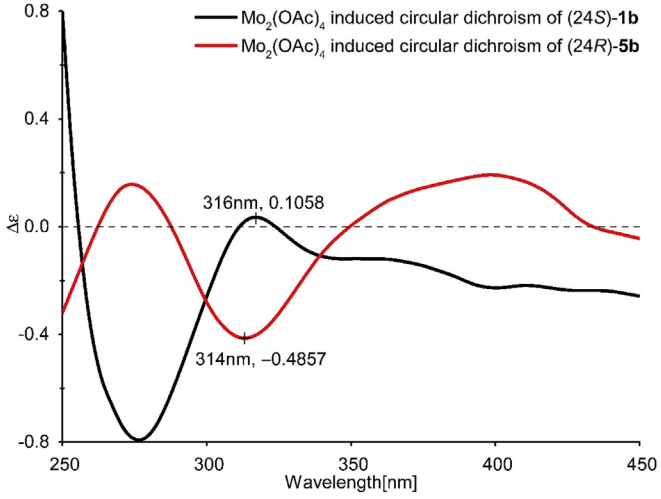

Fig. 4. $Mo_2(OAc)_4$-induced ECD spectra of compounds **1b** and **5b** in DMSO solution.

that the aldehyde group 30-CHO was located at C-14 (Fig. 2). Thus, compound **10** was determined as 3-O-α-[(α-L-arabinopyranosyl)-(1 → 2)-β-D-glucopyranosyl]-25-hydroxy-24,30-dioxolanost-8-ene.

Hebecarposide K (**11**) had a molecular formula of $C_{42}H_{70}O_{12}$

Table 3
^{1}H NMR spectroscopic data for compounds **6**–**11** (δ in ppm, J in Hz, and 400 MHz).

No.	**6**[a]	**7**[a]	**8**[a]	**9**[b]	**10**[a]	**11**[a]
1α	1.58, m	1.58, m	1.42, m	1.42, m	1.38, m	1.44, m
1β	2.10, m	2.10, m	2.11, m	2.00, m	1.98, m	1.93, m
2α	1.78, m	1.91, m	1.80, m	2.05, m	2.02, m	2.03, m
2β	1.73, m	1.70, m	1.75, m	1.79, m	1.74, m	1.74, m
3α	3.50, br s	3.53, overlap	3.49, br s	3.93, br s	3.84, br s	3.77, br s
5α	1.65, m	1.78, m	1.65, m	1.80, m	1.81, m	1.77, m
6α	1.56, m	1.49, m	1.56, m	1.55, m	1.52, m	1.50, m
6β	1.65, m	1.61, m	1.65, m	1.65, m	1.62, m	1.66, m
7α	1.97, m	2.01, m	2.01, m	2.00, m	1.97, m	1.94, m
7β	2.08, m	2.07, m	2.10, m	2.13, m	2.08, m	2.08, m
11α	2.09, m	1.55, m	1.73, m	1.95, m	1.90, m	1.93, m
11β	2.23, m	2.15, m	2.24, m	2.12, m	2.17, m	2.14, m
12α	1.71, m	1.77, m	1.72, m	1.78, m	1.77, m	1.78, m
12β	2.22, m	2.15, m	2.26, m	1.96, m	1.90, m	2.10, m
15α	2.03, m	2.10, m	2.20, m	2.30, m	2.30, m	2.30, m
15β	1.58, m	1.51, m	1.55, m	1.58, m	1.58, m	1.61, m
16α	1.35, m	1.35, m	1.45, m	2.13, m	2.15, m	2.14, m
16β	2.01, m	1.97, m	2.07, m	2.42, m	2.41, m	2.40, m
17α	1.51, m	1.51, m	1.52, m	1.61, m	1.55, m	1.52, m
18β	0.83, s	0.83, s	0.81, s	0.81, s	0.76, s	0.78, s
19β	1.06, s	1.06, s	1.06, s	1.10, s	1.09, s	1.04, s
20β	1.49, m	1.49, m	1.47, m	1.47, m	1.50, m	1.47, m
21α	0.95, d (5.9)	0.95, d (6.0)	0.94, d (6.1)	0.95, d (5.9)	0.81, d (6.4)	0.90, d (6.8)
22a	1.25, m	1.23, m	1.41, m	1.55, m	1.60, m	1.51, m
22b	1.48, m	1.50, m	1.77, m	2.00, m	2.01, m	1.76, m
23a	1.79, m	1.79, m	2.64, m	2.94, m	2.92, m	2.93, m
23b	1.41, m	1.49, m	2.62, m	2.92, m	2.85, m	2.90, m
24β	3.22, m	3.21, m				
26	1.16, s	1.16, s	1.29, s	1.57, s	1.56, s	1.56, s
27	1.13, s	1.13, s	1.29, s	1.57, s	1.56, s	1.56, s
28β	0.98, s	0.98, s	0.98, s	1.22, s	1.22, s	1.27, s
29α	0.91, s	0.91, s	0.91, s	0.87, s	0.87, s	0.89, s
30a		3.47, overlap		3.97, d (10.2)	10.16, s	1.06, s
30b		3.36, overlap		3.76, d (10.2)		
1′	4.30, d (7.7)	4.30, d (7.7)	4.27, d (7.8)	4.98, overlap	4.85, d (7.1)	4.80, overlap
2′	3.17, m	3.18, m	3.18, m	4.28, m	4.34, m	4.27, m
3′	3.38, m	3.35, m	3.36, m	4.32, m	4.33, m	4.26 m
4′	3.26, m	3.27, m	3.26, m	4.16, dd (9.0, 8.8)	4.15, dd (9.0, 9.0)	4.15, dd (9.0, 9.0)
5′	3.24, m	3.21, m	3.21, m	3.89, ddd (9.0, 5.6, 2.5)	3.84, ddd (9.0, 5.4, 2.5)	3.85, ddd (9.0, 5.2, 2.5)
6′a	3.66, dd (11.8, 5.6)	3.66, dd (11.8, 5.3)	3.66, dd (11.8, 5.7)	4.35, dd (12.1, 5.6)	4.36, m	4.33, dd (11.5, 5.2)
6′b	3.86, dd (11.8, 2.0)	3.86, dd (11.8, 2.1)	3.87, dd (11.8, 1.9)	4.56, dd (12.1, 2.5)	4.54, dd (12.1, 2.5)	4.51, dd (11.5, 2.5)
1″				6.50, s	6.66, s	6.54, s
2″				4.80, dd (3.1, 1.2)	4.78, dd (3.4, 0.9)	4.80, m
3″				4.60, dd (9.3, 3.1)	4.52, dd (9.6, 3.4)	4.53, dd (9.3, 3.4)
4″				4.26, m	4.28, m	4.28, m
5″				4.74, dd (9.3, 6.2)	4.75, dd (9.4, 6.1)	4.73, dd (9.4, 6.2)
6″				1.72, d (6.2)	1.68, d (6.1)	1.70, d (6.2)

[a] Recorded in methanol-d_4.
[b] Recorded in pyridine-d_5.

based on the HRESIMS peak at m/z 789.4764 $[M + Na]^+$ (calcd. for $C_{42}H_{70}O_{12}Na^+$, 789.4765) and ^{13}C NMR data. The NMR spectroscopic data (Tables 3 and 4) of **11** exhibited some similarities to those of **10**, but differed in the presence of a methyl group (δ_H 1.04, s, H$_3$-30; δ_C 24.8, C-30) in **11**, replacing the aldehyde group (δ_H 10.16, s, H-30; δ_C 201.4, C-30) in **10**. Thus, **11** is a 30-deoxy derivative of **10**. The HMBC cross peaks of H$_3$-30 (δ_H 1.06, s) to C-8 (δ_C 133.6), C-13 (δ_C 45.1), C-14 (δ_C 50.6), and C-15 (δ_C 31.6) confirmed the location of the methyl group 30-CH$_3$ at C-14 (Fig. 2). Thus, hebecarposide K (**11**) was identified as 3α-[α-L-arabinopyranosyl-(1 → 2)-(β-D-glucopyranosyl)-oxy]-25-hydroxy-24-oxolanost-8-ene.

Hebecarposides A–K (**1**–**13**) were evaluated for their anti-proliferative activities against five human cancer cell lines SMMC-7721, HL-60, SW480, MCF-7, and A-549, and a normal epithelial cell line BEAS-2B, and cis-platin was used as a positive control. As shown in Table 5, compounds **1**–**13** did not show significant anti-proliferative activities against the normal epithelial cell line BEAS-2B ($IC_{50} > 40$ μM), suggesting that all of them have no general cytotoxity. Interestingly, hebecarposides C (**3**), D (**4**), G (**7**), and K (**11**) selectively inhibited the proliferation of HL-60 and SMMC-7721 cell lines with IC_{50} values ranging from 13.52 to 35.89 μM. Hebecarposides C (**3**) and D (**4**) showed more potent anti-proliferative activities against A-549 cell lines with IC_{50} values of 18.64 ± 0.52 and 27.59 ± 3.21 μM, respectively, than the positive control, *cis*-platin ($IC_{50} = 28.23 \pm 2.95$ μM). While, hebecarposides C (**3**) and H (**7**) exhibited more potent inhibitory activities against the proliferation of MCF-7 ($IC_{50} = 22.15 \pm 1.02$ and 27.74 ± 1.29 μM, respectively) than the positive control ($IC_{50} = 35.02 \pm 2.17$ μM). Analysis of the structure-activity of **1**–**13** revealed that the oxidation state of C-30 plays an important role in the anti-proliferative activity of lanost-8-ene glycosides, and 30-CH$_2$OH and 30-CH$_3$ may be the active groups. The above data may provide a basis for the further investigation and optimization of lanost-8-ene type triterpene glycosides as an anti-proliferative agent for tumors, and extensive studies are required for their structure-activity relationship.

Table 4
^{13}C NMR spectroscopic data for compounds **6**–**11** (100 MHz).

No.	**6**[a]	**7**[a]	**8**[a]	**9**[b]	**10**[a]	**11**[a]
1	30.6	31.4	30.5	30.9	30.5	30.9
2	22.3	22.5	22.3	21.9	22.2	22.7
3	82.0	81.5	82.0	79.2	80.8	81.4
4	38.3	38.3	38.3	37.8	37.7	37.6
5	45.7	45.8	45.7	45.7	45.7	46.1
6	19.4	19.5	19.4	19.3	19.0	19.1
7	28.5	29.9	28.5	29.1	28.3	28.7
8	128.8	132.9	129.0	123.9	122.3	133.6
9	141.9	138.6	141.6	137.0	145.1	135.9
10	38.7	38.6	38.7	38.2	38.6	37.7
11	23.4	21.9	23.4	20.8	22.7	21.7
12	32.7	32.5	32.7	25.9	26.6	26.5
13	48.3	46.9	48.2	46.2	46.4	45.1
14	64.1	56.9	64.3	56.4	67.7	50.6
15	29.0	26.5	29.0	31.7	31.3	31.6
16	28.9	29.0	29.1	29.3	29.8	31.7
17	52.5	53.1	52.2	52.0	53.4	50.8
18	18.3	17.8	18.4	17.7	17.4	16.4
19	20.3	19.6	20.3	19.7	20.2	20.0
20	37.2	37.7	37.0	36.9	35.9	36.7
21	19.2	19.2	19.1	19.2	18.9	19.2
22	31.1	29.2	31.0	31.1	31.0	31.4
23	34.4	34.6	34.0	34.7	33.4	33.6
24	79.9	79.9	218.0	216.8	216.7	216.9
25	74.0	74.0	78.1	77.1	77.1	77.2
26	25.8	25.8	26.9	27.6	27.7	27.6
27	25.1	25.1	26.9	27.7	27.7	27.7
28	29.1	29.1	29.1	28.9	29.2	29.2
29	23.0	23.0	23.0	23.4	23.4	23.5
30	180.5	68.6	181.2	68.1	201.4	24.8
1′	101.6	101.1	101.6	99.2	100.7	101.1
2′	75.2	75.4	75.2	76.6	76.1	77.3
3′	78.2	78.4	78.3	80.0	80.2	80.6
4′	72.1	72.1	72.2	72.7	72.6	72.7
5′	78.0	78.0	78.0	78.8	78.7	78.5
6′	63.2	63.2	63.2	63.2	63.3	63.4
1″				101.3	101.6	101.8
2″				72.9	72.8	72.8
3″				72.0	73.4	73.2
4″				74.5	74.3	74.3
5″				69.9	69.6	69.8
6″				19.1	19.1	19.2

[a] Recorded in methanol-d_4.
[b] Recorded in pyridine-d_5.

3. Conclusions

A phytochemical investigation on the leaves of *L. ovalifolia* var. *hebecarpa* led to the isolation of eleven previously undescribed lanostane triterpene glucosides, hebecarposides A–K (**1**–**11**), and two known analogues, lyonifolosides L (**12**) and O (**13**). The structures of hebecarposides A–K (**1**–**11**) were established by extensive spectroscopic analysis, $Mo_2(OAc)_4$–induced ECD, and chemical methods. Thirteen lanostane triterpene glucosides were evaluated for their antiproliferative activities against five cancer cell lines and a normal cell line, and all of them did not show general cytotoxity to the normal cell line BEAS-2B. Hebecarposides C (**3**), D (**4**), G (**7**), and K (**11**) selectively inhibited the proliferation of cancer cell lines. Preliminary structure-activity-relationship analysis revealed that the oxidation state of C-30 plays an important role in the antiproliferative activity of lanost-8-ene glycosides, and 30-CH_2OH and 30-CH_3 may be the active groups. This is the first report of lanostane-type triterpene glycosides from *L. ovalifolia* var. *hebecarpa*, and lanostane triterpene glycosides may be served as a chemotaxonomic marker for the genus of *Lyonia*.

4. Experimental

4.1. General experimental procedures

Optical rotations were measured with a Rudolph Autopol IV automatic. The ECD spectra were obtained on a JASCO J–80 spectrometer. 1D and 2D NMR spectra were recorded on a Bruker AM–400 spectrometer with referencing to the residuals of ^1H (δ_H 3.31 for methanol-d_4 or δ_H 7.19 for pyridine-d_5) or ^{13}C (δ_C 49.2 for methanol-d_4 or δ_C 123.9 for pyridine-d_5). HRESIMS were acquired on a Bruker micrOTOF II spectrometer. Semi-preparative HPLC was accomplished on a Dionex 680 system with a UV detector using a reversed-phased (RP) C_{18} column (5 μm, 10 × 250 mm, Welch Ultimate XB–C_{18}). GC was analyzed using an Agilent 7820A gas chromatography and capillary column (30 m × 0.25 mm × 0.5 μm, Welch WM-1). The cytotoxicity assay was performed using a Multiskan FC multifunctional microplate reader.

4.2. Plant material

The leaves of *Lyonia ovalifolia* var. *hebecarpa* (Franch. ex F.B. Forbes & Hemsl.) Chun (Ericaceae) were collected at altitude about 2000 m, latitude 28°26′29″ North and longitude 120°8′59″ East, Jinyun County, Zhejiang Province, China, in June 2015, and authenticated by Professor Bing-Yang Ding at Wenzhou University. A voucher specimen (No. 2015-0616) has been deposited at School of Pharmacy, Tongji Medical College, Huazhong University of Science and Technology.

4.3. Extraction and isolation

The air-dried leaves of *L. ovalifolia* var. *hebecarpa* (50 Kg) were extracted with 95% aqueous EtOH (3 × 70 L, each 24 h) at 45 °C. After the removal of the solvent under the reduced pressure, the crude extract (9.2 Kg) was suspended in H_2O (65 L) and then partitioned with petroleum ether (6 × 10 L) and chloroform (6 × 10 L). The chloroform extract (5.2 Kg) was subjected to a silica gel (16.5 Kg, 100–200 mesh) column chromatography (CC) and eluted with CH_2Cl_2–MeOH (50:1 to 0:1, v/v) to afford nine fractions Fr.1–Fr.9. Fr.4 (43.5 g) was fractionated by an RP-C_{18} MPLC eluting

Table 5
Anti-proliferative activities of compounds **1**–**13** against five cancer cell lines and one normal cell line (IC_{50} in μM)[a,b].

Compound	HL-60	A-549	SMMC-7721	MCF-7	SW480	BEAS-2B	Highest index of selectivity[c]
3	16.93 ± 0.29	18.64 ± 0.52	17.79 ± 0.53	22.15 ± 1.02	33.32 ± 1.74	>40	>2.4
4	16.55 ± 0.30	27.59 ± 3.21	18.59 ± 1.14	>40	>40	>40	>2.4
7	13.52 ± 0.36	>40	35.89 ± 1.10	27.74 ± 1.29	>40	>40	>3.0
11	25.60 ± 0.25	>40	24.88 ± 1.64	>40	>40	>40	>0.6
cis-platin[d]	3.42 ± 0.17	28.23 ± 2.95	13.23 ± 1.17	35.02 ± 2.17	26.90 ± 1.93	>40	>11.7

[a] Other compounds: IC_{50} > 40 μM.
[b] IC_{50} values are presented as the means ± SD (n = 3).
[c] The "Highest index of selectivity" is the ratio of the IC_{50} value for the Beas-2B cell line over the lowest cancer cell IC_{50} value.
[d] Positive control.

with MeOH–H_2O (from 20:80 to 100:0, v/v) to generate a major fraction Fr.4D (10.2 g). Fr.4D was applied to a Sephadex LH–20 column (MeOH) to obtain three subfractions Fr.4D1–Fr.4D3. Compounds **7** (7.6 mg, $t_R = 38.1$ min) and **12** (127.5 mg, $t_R = 33.5$ min) were obtained from Fr.4D1 (200 mg) by a semipreparative HPLC eluting with MeCN–H_2O (50:50, v/v 1.5 mL/min). Subfraction Fr.4D2 (48.6 mg) was separated by a semipreparative HPLC (MeCN–H_2O, 80:30, v/v, 1.5 mL/min) to give compound **8** (12.2 mg, $t_R = 26.6$ min). Compounds **1** (12.0 mg, $t_R = 26.6$ min), **2** (7.0 mg, $t_R = 25.5$ min), and **5** (120.6 mg, $t_R = 24.5$ min) were isolated from Fr.4D3 (142 mg) by a semipreparative HPLC (MeCN–H_2O, 70:30, v/v, 1.5 mL/min). Fr.5 (129.5 g) was chromatographed over an RP-C_{18} MPLC eluting with MeOH–H_2O (from 20:80 to 100:0, v/v) to obtain a major fraction Fr.5C (2.7 g). Fr.5C was applied to a Sephadex LH-20 column (MeOH) to afford five subfractions (Fr.5C1–Fr.5C5). Compound **13** (15.1 mg, $t_R = 33.3$ min) was obtained from Fr.5C1 (148.7 mg) by a semipreparative HPLC (MeCN–H_2O, 80:20, v/v, 1.5 mL/min). Compounds **10** (12.6 mg, $t_R = 24.3$ min) and **11** (7.0 mg, $t_R = 38.2$ min) were isolated from Fr.5C2 (102.5 mg) by a semipreparative HPLC (MeCN–H_2O, 80:20, v/v, 1.5 mL/min). Purification of Fr.5C3 (14.2 mg) by a semipreparative HPLC (MeCN–H_2O, 67:33, v/v, 1.5 mL/min) yielded compound **9** (2.6 mg, $t_R = 35.3$ min). Fraction Fr.5C4 (102.3 mg) was separated by a semipreparative HPLC (MeCN–H_2O, 80:20, v/v, 1.5 mL/min) to give compound **3** (3.6 mg, $t_R = 33.3$ min). Further purification of fraction Fr.5C5 (248.6 mg) by a semipreparative HPLC (MeCN–H_2O, 80:20, v/v, 1.5 mL/min) afforded compounds **4** (20.0 mg, $t_R = 22.8$ min) and **6** (7.0 mg, $t_R = 20.6$ min).

4.3.1. Hebecarposide A (**1**)

White amorphous power; $[\alpha]_D^{25}$ −85 (*c* 0.4, MeOH); ^{1}H NMR and ^{13}C NMR data, see Tables 1 and 2; HRESIMS *m/z* 645.3978 $[M + Na]^+$ (calcd for $C_{35}H_{58}O_9Na$, 645.3979).

4.3.2. Hebecarposide B (**2**)

White amorphous power; $[\alpha]_D^{25}$ −22 (*c* 0.1, MeOH); ^{1}H NMR and ^{13}C NMR data, see Tables 1 and 2; HRESIMS *m/z* 645.3966 $[M + Na]^+$ (calcd for $C_{35}H_{58}O_9Na$, 645.3979).

4.3.3. Hebecarposide C (**3**)

White amorphous power; $[\alpha]_D^{25}$ −12 (*c* 0.4, MeOH); ^{1}H NMR and ^{13}C NMR data, see Tables 1 and 2; HRESIMS *m/z* 631.4193 $[M + Na]^+$ (calcd for $C_{35}H_{60}O_8Na$, 631.4186).

4.3.4. Hebecarposide D (**4**)

White amorphous power; $[\alpha]_D^{25}$ −20 (*c* 1.1, MeOH); ^{1}H NMR and ^{13}C NMR data, see Tables 1 and 2; HRESIMS *m/z* 661.4289 $[M + Na]^+$ (calcd for $C_{36}H_{62}O_9Na$, 661.4292).

4.3.5. Hebecarposide E (**5**)

White amorphous power; $[\alpha]_D^{25}$ −15 (*c* 0.3, MeOH); ^{1}H NMR and ^{13}C NMR data, see Tables 3 and 4; HRESIMS *m/z* 645.4007 $[M + Na]^+$ (calcd for $C_{35}H_{58}O_9Na$, 645.3979).

4.3.6. Hebecarposide F (**6**)

White amorphous power; $[\alpha]_D^{25}$ −7 (*c* 0.4, MeOH); ^{1}H NMR and ^{13}C NMR data, see Tables 3 and 4; HRESIMS *m/z* 675.4136 $[M + Na]^+$ (calcd for $C_{36}H_{60}O_{10}Na$, 675.4084).

4.3.7. Hebecarposide G (**7**)

White amorphous power; $[\alpha]_D^{25}$ −65 (*c* 1.5, MeOH); ^{1}H NMR and ^{13}C NMR data, see Tables 3 and 4; HRESIMS *m/z* 661.4316 $[M + Na]^+$ (calcd for $C_{36}H_{62}O_9Na$, 661.4292).

4.3.8. Hebecarposide H (**8**)

White amorphous power; $[\alpha]_D^{25}$ −23 (*c* 0.2, MeOH); ^{1}H NMR and ^{13}C NMR data, see Tables 3 and 4; HRESIMS *m/z* 673.3913 $[M + Na]^+$ (calcd for $C_{36}H_{58}O_{10}Na$, 673.3928).

4.3.9. Hebecarposide I (**9**)

White amorphous power; $[\alpha]_D^{25}$ −82 (*c* 0.2, MeOH); ^{1}H NMR and ^{13}C NMR data, see Tables 3 and 4; HRESIMS *m/z* 805.4705 $[M + Na]^+$ (calcd for $C_{42}H_{70}O_{13}Na$, 805.4714).

4.3.10. Hebecarposide J (**10**)

White amorphous power; $[\alpha]_D^{25}$ −188 (*c* 0.6, MeOH); ^{1}H NMR and ^{13}C NMR data, see Tables 3 and 4; HRESIMS *m/z* 803.4526$[M + Na]^+$ (calcd for $C_{42}H_{68}O_{13}Na$, 803.4558).

4.3.11. Hebecarposide K (**11**)

White amorphous power; $[\alpha]_D^{25}$ −27 (*c* 0.4, MeOH); ^{1}H NMR and ^{13}C NMR data, see Tables 3 and 4; HRESIMS *m/z* 789.4764$[M + Na]^+$ (calcd for $C_{42}H_{70}O_{12}Na$, 789.4765).

4.4. Acid hydrolysis and determination of the absolute configuration of sugar moieties of compounds **1**–**11**

Compound **1** (0.5 mg) was added to 1.5 mL 2 mM HCl, and the mixture was stirred for 6 h at 80 °C. After cooling to the room temperature, the reaction mixture was extracted with EtOAc (3 × 2.0 mL), and the aqueous layer was evaporated to dryness. The dried sugar residue was dissolved in 0.2 mL anhydrous pyridine, and then 0.2 mg L-cysteine methyl ester hydrochloride was added to the solution. The mixture was stirred at 60 °C for 1.5 h, subsequently, 0.1 mL *N*-trimethylsilylimidazole was added, and stirred at 60 °C for another 1.5 h. The reaction mixture was suspended in 1.0 mL H_2O and extracted with *n*-hexane (3 × 1.0 mL). The layer of *n*-hexane was directly analyzed by GC with a WM-1 capacity column. Nitrogen was used as a carrier gas at a flow rate of 1.0 mL/min. Flame ionization detector (FID) and injection were set at 250 °C. The split ratio was 10:1 and the injection volume was 1 μL. The oven temperature was programmed as follows: initial temperature at 230 °C for 5 min, increased to 270 °C at 10 °C/min, and held 3.0 min at the final temperature. In the same way, the trimethylsilylthiazolidine derivatives of the standards D- and L-arabinose were prepared and analyzed by GC. The GC retention times of the trimethylsilylthiazolidine derivatives of the hydrate of **1**, L- and D-arabinose were 8.83, 8.82, and 9.13 min, respectively, indicating the presence of L-arabinose in **1**.

In the same way, compounds **2**–**11** were hydrolyzed by 2 mM HCl, and the trimethylsilylthiazolidine derivatives of the hydrates of **2**–**11**, standards D-, L-glucose, and L-rhamnose were prepared. The trimethylsilylthiazolidine derivatives of the hydrates of compounds **2**, **3**, and **5** gave GC retention times at 8.88, 8.90, and 8.84 min, respectively, indicating the presence of L-arabinose. Detection conditions of the derivatives of standards D-, L-glucose, L-rhamnose, and hydrates of compounds **4** and **6**–**11** were different at column temperature: initially 220 °C for 5 min, raised to 270 °C at 5 °C/min, and kept 10 min. The GC retention times of the derivatives of standards D-, L-glucose, and L-rhamnose were 13.35, 13.85, and 13.56 min, respectively. The trimethylsilylthiazolidine derivatives of the hydrates of compounds **4** and **6**–**8** showed GC retention times at 13.30, 13.34, 13.35, and 13.31 min, respectively, indicating the presence of D-glucose. Two sugars in compounds **9**–**11** were determined to be D-glucose and L-rhamnose by the GC retention times of their trimethylsilylthiazolidine derivatives at 13.44 and 13.66 min (**9**), 13.34 and 13.67 min (**10**), and 13.33 and 13.64 min (**11**), respectively.

4.5. Preparation of the aglycone of compounds **1** and **5**

A solution of compound **1** (5.2 mg) in 0.5 mL MeOH was added 40 μL 0.6 mM TsOH·H_2O in MeOH, and the mixture was stirred at 65 °C for 72 h. After the removal of MeOH by evaporation, the reaction mixture was diluted with 3.0 mL H_2O and extracted with EtOAc (3 × 1.0 mL). The EtOAc extract was subjected to a silica gel CC (200–300 mesh) eluting with a CH_2Cl_2–CH_3OH (from 50:1 to 20:1, v/v) gradient system to yield the aglycone **1a** (2.4 mg). In the same way, the aglycone **5a** (3.6 mg) was prepared by the hydrolysis of compound **5** (5.0 mg).

4.5.1. Hebecarpolic acid A (**1a**)

White power; $[\alpha]_D^{25}$ −62 (*c* 0.3, MeOH); ^{1}H NMR and ^{13}C NMR data, see Tables 1 and 2; HRESIMS *m/z* 513.3561 $[M + Na]^+$ (calcd. for $C_{30}H_{50}O_5Na$, 513.3556).

4.5.2. Hebecarpolic acid E (**5a**)

White power; $[\alpha]_D^{25}$ −41 (*c* 0.1, MeOH); ^{1}H NMR and ^{13}C NMR data, see Tables 1 and 2; HRESIMS *m/z* 513.3553 $[M + Na]^+$ (calcd. for $C_{30}H_{50}O_5Na$, 513.3556).

4.6. Preparation of the methyl esters of compounds **1a** and **5a**

A mixture of **1a** (2.4 mg) and K_2CO_3 (1.0 mg) in 0.5 mL anhydrous DMF was added 4.6 μL MeI, and then the mixture was stirred at room temperature for 2 h. The reaction mixture was quenched with Na_2SO_3 (0.5 M), diluted with 1.0 mL H_2O, and extracted with EtOAc (3 × 1.0 mL). After concentration, the EtOAc extract was subjected to a silica gel CC (200–300 mesh) eluting with a CH_2Cl_2–CH_3OH (from 50:1 to 30:1, v/v) gradient system to yield the methyl ester **1b** (1.8 mg). In the say way, the methyl ester **5b** (2.4 mg) was prepared by the methylation of compound **5a**.

4.6.1. Hebecarpolic acid A methyl ester (**1b**)

White power; $[\alpha]_D^{25}$ −51 (*c* 0.1, MeOH); ^{1}H NMR and ^{13}C NMR data, see Tables 1 and 2; HRESIMS *m/z* 527.3729 $[M + Na]^+$ (calcd. for $C_{31}H_{52}O_5Na$, 527.3712).

4.6.2. Hebecarpolic acid E methyl ester (**5b**)

White power; $[\alpha]_D^{25}$ −35 (*c* 0.1, MeOH); ^{1}H NMR and ^{13}C NMR data, see Tables 1 and 2; HRESIMS *m/z* 527.3718 $[M + Na]^+$ (calcd. for $C_{31}H_{52}O_5Na$, 527.3712).

4.7. Determination of the absolute configuration of the 24,25-diol moieties in compounds **1b** and **5b**

According to the method previously described (Frelek et al., 2003; Gorecki et al., 2006, 2007; Snatzke et al., 1981), $Mo_2(OAc)_4$ was dissolved in dry DMSO to prepare a stock solution (1.0 mg/mL), and then the freshly prepared solution of $Mo_2(OAc)_4$ were added to compound **1b** (0.9 mg) in a molar ratio of 1.2:1. The $Mo_2(OAc)_4$-induced ECD (IECD) spectrum was immediately recorded every ten minutes until the IECD spectrum was constant. After subtracting the inherent ECD spectrum of **1b**, the $Mo_2(OAc)_4$-induced ECD spectrum of **1b** was prepared. The correlation between the absolute configuration of C-24 in **1b** and the Cotton effects in IECD spectrum was inferred using Snatzke's regulations (Snatzke et al., 1981). The absolute configuration of the 24,25-diol moiety in compound **5b** (0.8 mg) was determined in the same way.

4.8. Cytotoxicity assays

The cytotoxicity assays were performed according to the procedure previously described (Luo et al., 2012), and the IC_{50} values of the compounds were calculated by Reed and Muench method (Reed and Muench, 1938).

Acknowledgements

This work was supported financially by National Natural Science Foundation of China (U1703109, 81001368, and 31170323) and the Fundamental Funds for the Central Universities (HUST: 2016YXMS148). We thank the Analytical and Testing Center at Huazhong University of Science and Technology for ECD data analysis.

Appendix A. Supplementary data

Supplementary data associated with this article can be found in the online version, at https://doi.org/10.1016/j.phytochem.2018.03.012. These data include MOL files and InChiKeys of the most important compounds described in this article.

References

Adinolfi, M., Corsaro, M.M., Lanzetta, R., Mancino, A., Mangoni, L., Parrilli, M., 1993. Triterpenoid oligoglycosides from *Chionodoxa luciliae*. Phytochemistry 34, 773–778.

Aminin, D.L., Pislyagin, E.A., Menchinskaya, E.S., Silchenko, A.S., Avilov, S.A., Kalinin, V.I., 2014. Immunomodulatory and anticancer activity of sea cucumber triterpene glycosides. Stud. Nat. Prod. Chem. 41, 75–94.

Bukreyeva, T.V., Shavarda, A.L., Matusevich, O.V., Morozov, M.A., 2013. Ursane, oleanane and lupane triterpenoids in leaves of *Ledum palustre* (Ericaceae) from the North-West Russia. Rastitel'nye Resur. 49, 395–403.

Dai, S.J., Yu, D.Q., 2005. Triterpenoids of *Rhododendron anthopogonoide* Maxim. Zhongguo Tianran Yaowu 3, 347–349.

Duru, M.E., Tel, C.G., 2015. Biologically active terpenoids from mushroom origin: a review. Rec. Nat. Prod. 9, 456–483.

Editorial Committee of the Flora of China, Chinese Academy of Sciences, 1991. Flora of China, vol. 57. Science Press, Beijing, p. 30.

Frelek, J., Klimek, A., Ruskowska, P., 2003. Dinuclear transition metal complexes as auxiliary chromophores in chiroptical studies on bioactive compounds. Curr. Org. Chem. 7, 1081–1104.

Gorecki, M., Kaminska, A., Ruskowska, P., Suszczynska, A., Frelek, J., 2006. Dimolybdenum method for determination of the absolute configuration of *vic*-diols-foundations and developments. Pol. J. Chem. 80, 523–534.

Górecki, M., Jabłońska, E., Kruszewska, A., Suszczyńska, A., Urbańczyk-Lipkowska, Z., Gerards, M., Morzycki, J.W., Szczepek, W.J., Frelek, J., 2007. Practical method for the absolute configuration assignment of *tert*/*tert* 1,2-diols using their complexes with $Mo_2(OAc)_4$. J. Org. Chem. 72, 2906–2916.

Hamid, K., Alqahtani, A., Kim, M.S., Cho, J.L., Cui, P.H., Li, Ch, G., Groundwater, P.W., Li, G.Q., 2015. Tetracyclic triterpenoids in herbal medicines and their activities in diabetes and its complications. Curr. Top. Med. Chem. 15, 2406–2430.

Huang, X.Z., Liu, Y., Yu, S.S., Hu, Y.C., Qu, J., 2007. Triterpenoids from the roots of *Craibiodendron henryi* W. W. Smith. J. Integr. Plant Biol. 49, 1615–1618.

Isaka, M., Chinthanom, P., Sappan, M., Supothina, S., Vichai, V., Danwisetkanjana, K., Boonpratuang, T., Hyde, K.D., Choeyklin, R., 2017. Antitubercular activity of mycelium-associated *Ganoderma* lanostanoids. J. Nat. Prod. 80, 1361–1369.

Jin, Y.P., Yan, S., Liu, J.X., Yang, Y., Wang, Y.S., Wang, Y.P., 2014. Research progress on lanostane-type triterpenoids in plants of *Schisandraceae* and their pharmacologic. Zhongcaoyao 45, 137–143.

Kalinin, V.I., Avilov, S.A., Silchenko, A.S., Stonik, V.A., 2015. Triterpene glycosides of sea cucumbers (*Holothuroidea*, *Echinodermata*) as taxonomic markers. Nat. Prod. Commun. 10, 21–26.

Lee, I.K., Jung, J.Y., Yeom, J.H., Ki, D.W., Lee, M.S., Yeo, W.H., Yun, B.S., 2012. Fomitoside K, a new lanostane triterpene glycoside from the fruiting body of *Fomitopsis nigra*. Mycobiology 1, 76–78.

Luo, Z., Wang, F., Zhang, J., Li, X.Y., Zhang, M., Hao, X., Xue, Y., Li, Y., Horgen, F.D., Yao, G., Zhang, Y., 2012. Cytotoxic alkaloids from the whole plants of *Zephyranthes candida*. J. Nat. Prod. 75, 2113–2120.

Lv, X.J., Li, Y., Ma, S.G., Qu, J., Liu, Y.B., Li, Y.H., Zhang, D., Li, L., Yu, S.S., 2016. Antiviral triterpenes from the twigs and leaves of *Lyonia ovalifolia*. J. Nat. Prod. 79, 2824–2837.

Mamedova, R.P., Agzamova, M.A., Isaev, M.I., 2003. Triterpene glycosides of *Astragalus* and their genins. LXX. Orbicoside, the first lanostane glycoside from *Astragalus* plants. Chem. Nat. Compd. 39, 583–585.

Okwu, D.E., Offiong, O.N., 2009. Isolation and characterization of lanostane glycoside from the leaves of *Stachyterpheta jamaicensis* Linn Vahl. Int. J. ChemTech Res. 1, 1043–1047.

Ono, M., Toyohisa, D., Morishita, T., Horita, H., Yasuda, S., Nishida, Y., Tanaka, T., Okawa, M., Kinjo, J., Yoshimitsu, H., Nohara, T., 2011. Three new nortriterpene glycosides and two new triterpene glycosides from the bulbs of *Scilla scilloides*.

Chem. Pharm. Bull. 59, 1348–1354.
Ori, K., Kuroda, M., Mimaki, Y., Sakagami, H., Sashida, Y., 2003a. Norlanostane and lanostane glycosides from the bulbs of *Chionodoxa luciliae* and their cytotoxic activity. Chem. Pharm. Bull. 51, 92–95.
Ori, K., Koroda, M., Mimaki, Y., Sakagami, H., Sashida, Y., 2003b. Lanosterol and tetranorlanosterol glycosides from the bulbs of *Muscari paradoxum*. Phytochemistry 64, 1351–1359.
Reed, L.J., Muench, H., 1938. A simple method of estimating fifty percent end points. Am. J. Epidemiol. 27, 493–497.
Snatzke, G., Wagner, U., Wolff, H.P., 1981. Circulardichroism—LXXV[1]: cottonogenic derivatives of chiral bidentate ligands with the complex $[Mo_2(O_2CCH_3)_4]$. Tetrahedron 37, 349–361.
Tohtahon, Z., Xue, J., Han, J., Liu, Y., Hua, H., Yuan, T., 2017. Cytotoxic lanostane triterpenoids from the fruiting bodies of *Piptoporus betulinus*. Phytochemistry 143, 98–103.
Wang, C.F., Liu, Y.Z., Li, C.J., Chen, S.L., Qing, G.W., 2001. Study of chemical constituents from *Lyonia ovalifolia* var. *hebecarpa*. J. Henan Med. Univ. 36, 743–745.
Way, T.D., Tsai, S.J., Wang, C.M., Ho, C.T., Chou, C.H., 2014. Chemical constituents of *Rhododendron formosanum* show pronounced growth inhibitory effect on non-small-cell lung carcinoma cells. J. Agric. Food Chem. 62, 875–884.
Yao, G., Zhai, H., Wang, L., Qin, G., 2006. Research progress in chemical constituents and biological activities of *Pieris* plants (Ericaceae). Sci. Online 1, 286–290.
Zhang, M., Zhu, Y., Zhan, G., Shu, P., Sa, R., Lei, L., Xiang, M., Xue, Y., Luo, Z., Wan, Q., Yao, G., Zhang, Y., 2013. Micranthanone A, a new diterpene with an unprecedented carbon skeleton from *Rhododendron micranthum*. Org. Lett. 15, 3094–3097.
Zhang, M., Xie, Y., Zhan, G., Lei, L., Shu, P., Chen, Y., Xue, Y., Luo, Z., Wan, Q., Yao, G., Zhang, Y., 2015. Grayanane and leucothane diterpenoids from the leaves of *Rhododendron micranthum*. Phytochemistry 117, 107–105.
Zhou, J., Sun, N., Zhang, H., Zheng, G., Liu, J., Yao, G., 2017a. Rhodomollacetals A–C, PTP1B inhibitory diterpenoids with a 2,3:5,6-di-seco-grayanane skeleton from the leaves of *Rhododendron molle*. Org. Lett. 19, 5352–5355.
Zhou, J., Zhan, G., Zhang, H., Zhang, Q., Li, Y., Xue, Y., Yao, G., 2017b. Rhodomollanol A, a highly oxygenated diterpenoid with a 5/7/5/5 tetracyclic carbon skeleton from the leaves of *Rhododendron molle*. Org. Lett. 19, 3935–3938.
Zhou, J., Liu, J., Dang, T., Zhou, H., Zhang, H., Yao, G., 2018a. Mollebenzylanols A and B, highly modified and functionalized diterpenoids with a 9-benzyl-8,10-dioxatricyclo[5.2.1.$0^{1,5}$]decane core from *Rhododendron molle*. Org. Lett. 20, 2063–2066.
Zhou, J., Liu, T., Zhang, H., Zheng, G., Qiu, Y., Deng, M., Zhang, C., Yao, G., 2018b. Anti-inflammatory grayanane diterpenoids from the leaves of *Rhododendron molle*. J. Nat. Prod. 81, 151–161.